

Local phonon mode in a fermionic bath, and its relation to the Kondo effect

Balázs Dóra

Max-Planck-Institut für Physik Komplexer Systeme, Nothnitzer Str. 38, 01187 Dresden, Germany
(Dated: March 23, 2024)

We have studied the interplay of a local phonon mode embedded in a metallic host (Holstein impurity model) using Abelian bosonization. The phonon frequency softens, which takes place in two steps: first, their frequency starts softening, and acquires finite lifetime. Then oscillations disappear from the response, and two distinct, finite dampings characterize them. Similar behaviour shows up in the spin-boson model. Due to phonons, the electrons experience an attractive, dynamic interaction. As a result, the electronic charge response enhances similarly to the spin response in the Kondo model. The local electronic density of states develops a dip around zero frequency. Thus the chance of charge-Kondo effect emerges.

PACS numbers: 73.23.-b, 73.63.-b, 72.10.Fk

I. INTRODUCTION

Single impurity models have a long history¹, and our understanding has profited a lot from different reliable techniques. Numerical renormalization group, conformal field theory, Nozières' Fermi liquid description, Bethe ansatz solution and bosonization completed each other, and highlighted different aspects of the same problem. In many cases, the latter, being nonperturbative and analytic, was able to provide us with a transparent picture of the underlying physics². Its appeal is due to the elegance of analytic solution, being able to treat dynamic quantities as well (correlation functions), and the simplicity of the picture emerging from it.

Beyond electron-electron interaction, which is a basic ingredient in Kondo type models, another source of correlation is represented by phonons^{3,4,5,6,7,8}. They play a prominent role in explaining the conventional s-wave BCS superconductivity and the charge density wave formation in low dimensional systems. Their general feature is the generated dynamic interaction between the electrons, which, in essence, is attractive for small energy transfers.

In many strongly correlated systems, such as heavy fermions or valence fluctuation systems, lattice vibrations are known to couple strongly to electrons. The recent discovery of magnetically robust heavy fermion behaviour in filled skutterudite compound⁹ $\text{SmO}_4\text{Sb}_{12}$ renewed interest in Kondo phenomena with phononic origin^{10,11}. Both the specific heat coefficient and coefficient of the quadratic temperature dependence of the electrical resistivity were found to be almost independent of an applied magnetic field. Quantum dots, especially the ones based on single molecules (C_{60} for example¹²), also possess vibrational degrees of freedom, which will react to the electron transfer through them¹³. Therefore the properties of impurity models dominated by phonons are challenging. The applied methods should be able to treat dynamical properties, which rules out techniques as the Bethe ansatz.

Several theoretical investigation focused on electron transport in the presence of electron-phonon interaction,

mainly in the context of the single impurity Anderson-Holstein model. This model consists of an Anderson impurity with linear coupling to a local phonon mode⁴. Hewson and Newns considered its spinless version with a few electron in the system without explicit electron correlation^{14,15}. Later further studies based on the NRG (numerical renormalization group)^{4,5,11,16} and the non-equilibrium Keldysh formalism^{7,8} have been performed. These works reported about the softening of the local phonon mode, and the enhancement of the charge susceptibility. These phenomena point toward the realization of the charge-Kondo effect, caused by the degeneracy of zero and doubly occupied electron states.

In the present work, using Abelian bosonization, for the first time to our knowledge to attack the local electron-phonon problem, we can not only confirm the prediction of previous works, but also study analytically the specific heat, the phonon Green's function, the charge susceptibility and especially the local density of states. We follow the softening of phonons from weak to strong coupling, and connect the present problem with the underscreened Kondo model in magnetic field. As the electron-phonon coupling increases, phonon states with large occupation number start to play an important role even at very low temperatures, leading to a transition to a phonon distorted state only at infinitely strong coupling. Similar phenomenon reveals itself in the spin-boson model as well^{7,18}. Then, in contrast to NRG, where only a finite number of phonons can be taken into account, we can consider states with arbitrary phonons, and the crossover and the softening at arbitrary electron-phonon couplings.

II. THE MODEL

In real materials, electrons interact with each other explicitly through the Coulomb force and implicitly through phonons. In several cases, the resulting phase is well described by Landau's Fermi liquid theory with renormalized quasiparticle parameters due to interactions¹⁹. However, certain inhomogeneities like im-

purities, lattice imperfections are usually present, and exhibit a source of scattering. When these are of electronic origin, spin-Kondo physics is evoked¹. The local perturbations can also show up in the form of local lattice vibrations. This is why we have undertaken the study of spinless fermions interacting with a single, dispersionless Einstein phonon mode, mainly at zero temperature. This can be called the single impurity Holstein model, which is related to the Holstein model as the single impurity Anderson model is related to its periodic version. It also parallels to the one studied in Ref. 14,15 in the same way as the single impurity Woll model²⁰ is connected with the Anderson model¹. A similar model has been studied¹⁰ describing the coupling of a local Einstein phonon to conduction electrons by the numerical renormalization group, with emphasis on the nature of the fixed points, and relations with the two-level Kondo effect have been revealed. The present model can also be relevant for the dynamical mean-field theory (DMFT) of the Holstein lattice model²¹, which maps it onto the Holstein impurity model. Coupling to acoustic phonons would also be a fruitful proposition, but the essence of physics is readily captured by the simplest model. When the coupling of the electron density to the phonon displacement field is isotropic, the model can be mapped onto a single branch of chiral fermions interacting with a single Einstein phonon only at the origin, and is suitable for Abelian bosonization. This mapping follows closely the one proposed in Ref. 22 for the Kondo model².

In the Hamiltonian language, the model is given by:

$$H = \int_{-L/2}^{L/2} dx \left[\frac{v}{2} \left(\frac{\partial \phi}{\partial x} \right)^2 + g Q \phi(0) \right] + \frac{P^2}{2m} + \frac{m \omega_0^2}{2} Q^2; \quad (1)$$

and only the radial motion of the particles is accounted for by chiral (right moving) fermion field²², $\phi(x) = \phi^+(x) \phi(x)$: is the normal ordered electron density, L is the length of the system, v is the Fermi velocity, g describes the local electron-phonon coupling, m and ω_0 are the phononic mass and frequency, respectively, Q and P are the phonon displacement field and momentum conjugate to it.

In spirit, this model is similar to the underscreened Kondo model in a magnetic field (which quenches the remaining degrees of freedom) with phonons replacing the impurity spin, since the phonon displacement field (Q) can take any real values, while the electron density trying to compensate it, is bounded, although states with a large number of bosons in the harmonic oscillator hardly contribute to the physics at low temperatures due to their high energy. The underscreened Kondo model in a magnetic field is governed by a Fermi liquid fixed point. We speculate that the model under study produces similar behaviour. When the magnetic field is switched off, the underscreened Kondo model shows singular Fermi liquid behaviour²³, whose analogue in the present case occurs at $g \rightarrow 1$. Since the charge degrees of freedom

are coupled to the local bosons, the possibility of observing the "underscreened" charge-Kondo effect opens³. The realization of the charge-Kondo effect has also been found in similar models^{24,25}. Our model is similar to the one describing a tunneling particle coupled to a fermionic environment²⁶. The model can be bosonized via^{27,28}

$$\phi(x) = \frac{1}{\sqrt{2}} \exp(i \frac{P}{4} \phi(x)) \quad (2)$$

to lead

$$H = \int_{-L/2}^{L/2} dx \left(\frac{v}{2} \left(\frac{\partial \phi}{\partial x} \right)^2 + \frac{g}{2} Q \phi(0) \right) + \frac{P^2}{2m} + \frac{m \omega_0^2}{2} Q^2; \quad (3)$$

If we integrated out the phonon degrees of freedom in Eq. (1) or (3), we would arrive to a local interaction between electrons, given by $2g^2/m(\omega_0^2 - \omega^2)$, ω is the energy transfer in the interaction. At low energies ($\omega < \omega_0$), this would lead to an effective attractive interaction, and the resulting Hamiltonian would coincide with the spin sector of the repulsive Woll impurity model^{20,29,30}, responsible for the spin-Kondo phenomenon. Hence our model is capable to show Kondo physics in the charge sector. This further strengthens our proposal for the charge-Kondo effect. Attractive local interactions has already provided us with similar phenomenon^{4,5}.

This resulting Hamiltonian (Eq. (3)) is similar to the Caldeira-Leggett Hamiltonian (CL), describing the dynamics of a particle coupled to dissipative environment³¹. However, the roles are reversed between oscillators and tunneling particle in Eq. (3) and in Ref. 31: our localized phonon represents the tunneling particle in CL language, while the bosonized (ϕ) fermionic field stands for the dissipative environment of CL, represented by harmonic oscillators. An important difference between the two models is the lack of renormalization of potential in CL, ensuring, that the coupling to reservoir solely introduces dissipation¹⁷. In our case, however, we expect the softening of the phonon mode due the interaction with fermions on physical ground, hence the renormalization of the phonon frequency plays an essential role as is testified later in Eq. (14), in addition to dissipation. Moreover, the properties of our original fermionic field must be obtained through Eq. (2), a difficulty which is never faced with in the Caldeira-Leggett model.

Our bosonized Hamiltonian (Eq. (3)) also shares similar properties with the spin-boson model, where a two-level system is coupled to a bosonic environment^{17,18}. There, assuming an Ohmic bath, at a finite value of the coupling of the boson-two-level system, a quantum phase transition has been identified. In our case, the bosonic bath is represented by the bosonized fermions, but the two-level system is replaced by a multi-level system, i.e. a harmonic oscillator. As a result, the obtained behaviour of our model differs from that found in the spin-boson model, although some dynamical features, connected with the oscillation frequency, are similar.

III. LIMITING CASES

The adiabatic limit ($\hbar \rightarrow 0$) is meaningful, if it is taken together with $m \rightarrow 1$, keeping $m \hbar_0^2 = \text{finite}$. The phonons kinetic energy vanishes, and only a static displacement is felt by the electrons. Hence, the model reduces to a simple scattering problem, although one has to minimize the total free energy of the system (electronic contribution + elastic energy $Q^2/2$) with respect to the frozen phonon displacement field to obtain the correct solution, which transforms our problem into a self-consistent mean-field theory, which is the exact solution in this limit. The free energy, subject to minimization with respect to Q , reads at $T = 0$ as

$$F = n_0 g Q \frac{2}{\pi} \int_0^{\pi/2} d\theta \arctan(gQ \cos \theta) + \frac{1}{2} Q^2; \quad (4)$$

which leads to the self-consistency equation for Q :

$$\frac{Q}{2gn_0} = \arctan(gQ); \quad (5)$$

where $n_0 = W$ is the average electron density per site. In the weak coupling limit, only the trivial solution exists ($Q = 0$), as opposed to standard mean-field treatments of the Holstein lattice model³². As g exceeds $g_c = \frac{\pi}{2n_0}$, a non-trivial solution shows up, which minimizes the free energy. This behaves as $Q = \frac{\pi}{6(g - g_c)} \propto \frac{1}{g - g_c}$ close to g_c , and $Q = gn_0$ as g grows to infinity. For $g > g_c$, the electrons feel a local scattering center with strength $V = gQ$, and the local electronic density of states is expected to be suppressed³³ close to zero frequency as $1 = (1 + (V/\hbar)^2)$. Complete suppression occurs only for $g \rightarrow \infty$. Phonons lose their dynamics completely. However, when quitting the strict adiabatic limit, the displacement field is not frozen anymore, quantum corrections are expected to destroy ordering. In essence, this is similar to the large N limit of impurity models⁴ (N denotes the spin degeneracy), where a true phase transition occurs only in the $1/N = 0$ limit. Note, that similar calculation applies to the adiabatic limit of the Anderson-Holstein impurity model as well.

In the anti-adiabatic limit, $\hbar \rightarrow \infty$ while keeping the ratio $g = \hbar_0^2$ finite, the phonons react instantaneously to the electrons, leading to non-retarded interaction between the densities as

$$H_{\text{int}} = \frac{g^2}{2m \hbar_0^2} (n - n_0)^2; \quad (6)$$

where n is the charge density of electrons at the origin. Had we chosen spinful fermions, the resulting model would coincide with the negative U Woll model^{20,30} ($U = g^2/m \hbar_0^2$). In the spinless case, this again reduces to potential scattering with strength $V = g^2(2n_0 - 1)/2m \hbar_0^2$. Again, the local density of states is expected to be suppressed close to zero frequency, similarly to the adiabatic case.

Finally by taking the atomic or zero bandwidth limit, which also describes the infinite coupling case ($g \rightarrow \infty$), the phonons couple only to an isolated electron:

$$H_{\text{at}} = c^\dagger c (E + gQ) + \frac{p^2}{2m} + \frac{m \hbar_0^2}{2} Q^2; \quad (7)$$

where E is the c -level energy. This model is known as the independent boson model³³. Since the electron number operator ($c^\dagger c$) is conserved, most of the physical quantities can trivially be evaluated. However, the electron Green's function does not belong to this class. After a unitary transformation ($U = \exp(-igP^\dagger c = m \hbar_0^2)$), this can be evaluated exactly as

$$G_{\text{at}}(t) = \hbar c(t) c^\dagger i = (1 - \hbar c i) \exp(-iEt) \frac{g^2}{2m \hbar_0^2} t + \frac{g^2}{m \hbar_0^2} D_Q(t) \hbar Q^2 i; \quad (8)$$

Here the first term is the renormalized c -level Green's function, $\hbar Q^2 i = 1/2m \hbar_0^2$ is the mean square value of the displacement field, being independent of the coupling in this case. Finally, $D_Q(t)$ is the Green's function of the displacement field Q given by

$$D_Q(t) = \hbar Q^2 i \exp(-i|t|): \quad (9)$$

From this, one can evaluate the density of states, which reads as

$$\rho_{\text{at}}(\epsilon) = \exp\left(-\frac{\epsilon^2}{g^2}\right) \sum_{n=0}^{\infty} \frac{1}{n!} (\epsilon - E + \frac{1}{2} n \hbar_0^2) \quad (10)$$

with $\epsilon = \epsilon - E + \frac{1}{2} n \hbar_0^2$. Compared to the original density of states with $g = 0$, where a single Dirac-delta peak contains all the spectral weight, it is now distributed non-uniformly among infinite number of peaks. In general, most of the spectral weight is concentrated around $\epsilon = E$ for a finite g as well. In the weak coupling limit ($g \rightarrow 0$), the weight decreases monotonically with n . For strong coupling ($g \rightarrow \infty$), the largest weights are still distributed around $\epsilon = E$, which means that the $n = 0$ terms are the most dominant in the sum. These weights are proportional to $1/n!$. From this, one can conclude, that by increasing g to move from weak to strong coupling, terms with $n \propto 1/g^2$ contain the largest spectral weights, which, however decreases as $1/g^2$. This means that increasing amount of spectral weight is transferred away from the central region, hence the local density of states is suppressed due to phonons, as borns out from the above three limiting cases. It is only suppressed to zero for infinitely strong coupling g .

IV. SOFTENING OF THE PHONON

To determine the dynamics of our system, we start with the evaluation of the Green's function of the phonon

displacement field, defined by

$$D_Q(\mathbf{r}) = \hbar T Q(\mathbf{r}) Q(0) i; \quad (11)$$

whose Matsubara form can easily be calculated using the standard diagrammatic technique from Eq. (3), which yields to

$$D_Q(i\omega_m) = \frac{1}{m} \frac{1}{\omega_m^2 + \omega_0^2} \frac{1}{2g} \frac{1}{(i\omega_m)^2 + m}; \quad (12)$$

where $\omega_0 = 1/2v$, ω_m is the bosonic Matsubara frequency and

$$\chi(\omega_m) = \sum_{\mathbf{q} > 0} \frac{(v\mathbf{q})^2}{\omega_m^2 + (v\mathbf{q})^2} \quad (13)$$

is the local susceptibility of the fermions without the phonons. After analytic continuation to real frequencies, it is given by $\chi(\omega) = \chi(\omega + i0^+)$ for small frequencies, W is the cutoff or bandwidth, and the obtained formula holds regardless to the chosen cutoff procedure. Our Eq. (12) is exact for the Hamiltonian given by Eq. (3), no other diagrams are left to consider. However, the bosonization cutoff scheme renormalizes the coupling constant², and the impurity potential g needs to be replaced by the appropriate scattering phase shift. Since this is not a universal quantity (apart from the linear term), it depends on the regularization scheme, and we consider it to be replaced by the renormalized one onwards, as is standard in impurity models². The dynamics of the phonons can be inferred by investigating the pole structure of Eq. (12). The excitations energies become complex (i.e. finite lifetime or damping of phonon excitations) in the presence of finite coupling to the electrons, and are given by

$$\omega_p = i \frac{g}{\omega_0^2 + \omega_p^2} \frac{1}{4W} \quad (14)$$

with $\omega_p^2 = (g)^2/4W$. Below $\omega_0 < \omega_1 = 2W = \sqrt{4W^2 - \omega_0^2}$, the square root in Eq. (14) is real, hence the displacements reach their equilibrium in an oscillatory fashion within a time characterized by $\tau = \text{Im} \omega_p$. For higher frequencies, the phonon mode is completely softened, $\text{Re} \omega_p = 0$ (the square root becomes imaginary), the excitations have two different finite lifetimes or dampings determined from Eq. (14) between $\omega_1 < \omega_2 = \omega_0^2/4W$. Interestingly, the very same critical value ω_2 would be found, if we inserted the value of $g_c = \omega_0^2/m = 2n_0$ found in the extreme adiabatic limit (or self-consistent mean field theory) to $\omega_p^2 = (g)^2/4W$, which is, in turn, zero because $\omega_0 \rightarrow 0$. In this range, phonons can be excited with zero energy, and all the displacements are relaxed to equilibrium without oscillations. This relaxation slows down close to ω_2 . This region is very narrow, because for realistic values, $\omega_0 \ll W$, it shrinks as ω_0^4/W^3 . Similar relaxation characterizes two-level systems coupled to a bosonic bath^{17,18}. For higher values of g , our approach breaks down, it signals

lattice distortion with $\langle Q \rangle \neq 0$, as is indicated by the complete softening of the phonon mode. However, such a phenomenon is impossible in zero dimensional systems, and we ascribe it to bosonization. The explicit functional form of physical quantities on model parameters obtained by bosonization can deviate from the exact one. The phase shifts in impurity problems³⁴, the correlation exponents in Luttinger liquids determined via bosonization are only correct in the weak coupling limit². This and the previous argumentation suggests, that in reality, ω_2 should only be reached for $g \rightarrow 1$, but the complete softening predicted at ω_1 would take place at a finite value of g , and ω_2^2 only at small g . In the adiabatic limit, $(m \rightarrow 1, \omega_0 \rightarrow 0)$ also vanishes, and $\omega_1 = 0$.

We mention that such softening remains absent in the Caldeira-Leggett model due to the compensation of the potential renormalization there³¹. Similar phenomenon occurs in a two-level system, coupled to a bath of three dimensional phonons³⁵. The renormalized tunneling rate drops to zero only at infinitely strong coupling.

The softening of the phonon frequency was also found in the NRG treatment of the Anderson-Holstein impurity model^{4,5,16}, but this has only been followed in a moderate range of parameters. DMFT studies of the Holstein lattice model also revealed similar features²¹.

The general behaviour of the eigenfrequencies is sketched in Fig. 1. The phonon density of states contains

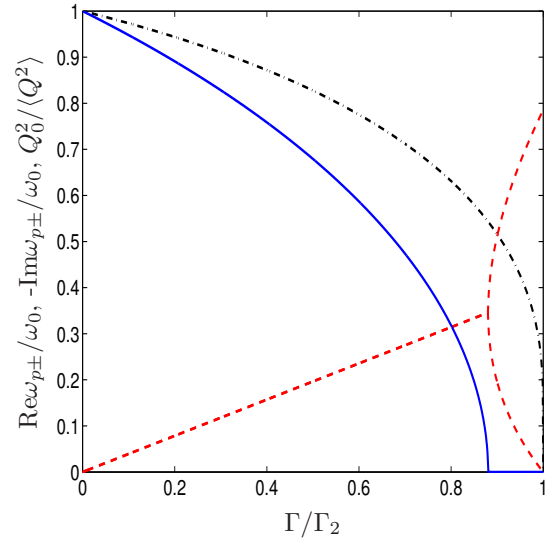


FIG. 1: (Color online) The real (blue solid line) and imaginary (red dashed line) part of the phonon excitation energies, and the inverse of the mean square value of the displacement field (black dashed-dotted line) are visualized as a function of the electron-phonon coupling for $W = \omega_0 = 2$. At ω_1 , the phonon mode is softened, but the excitations have finite lifetime. At ω_2 , the damping vanishes, the lifetime ($\tau = \text{Im} \omega_p$) diverges, and so does the mean square value of the displacement field.

two Lorentzians with resonance widths $-\text{Im} \omega_p$, centered around $\text{Re} \omega_p$. With increasing g , they become centered around the origin, and close to ω_2 , the one determined by ω_{p+} tends to ω_0 . This is reminiscent to what happens

in the channel anisotropic two channel Kondo model³⁶. In comparison with the underscreened Kondo model in a magnetic field, a similar divergence shows up in the localized electron density of states²³ with the onset of magnetic field. The very same role is played in our case by β_2 , which causes the divergence as $\beta_+ \rightarrow 0$. Softening of the phonon mode has been found by the numerical renormalization group as well⁴ in a similar model.

V. THERMODYNAMICS

The mean value of the displacement field is zero. The mean square value of the displacement field is calculated from Eq. (12) at $T = 0$ as

$$\langle Q^2 \rangle = \lim_{T \rightarrow 0} T \sum_m D_Q(\omega_m) = Q_0^2 \frac{2i\omega_0}{(\omega_+ - \omega_-)} \ln \frac{\omega_+}{\omega_-}; \quad (15)$$

where $Q_0^2 = 1/2m\omega_0$ is the value for $g = 0$. It is plotted in Fig. 1. As β_2 approaches β_+ , it diverges as

$$\frac{\langle Q^2 \rangle}{Q_0^2} \sim \frac{\omega_0}{2} \ln \frac{4}{\omega_0^2 (\beta_2 - \beta_+)}; \quad (16)$$

indicating the change in the $\langle Q \rangle = 0$ relation. This is traced back to the transition to the phonon distorted state at $g = 1$, as discussed below Eq. (14). Similar phenomenon has been observed in the spin-boson model^{17,18} at a finite value of the spin-boson coupling, assuming an Ohmic bath. However, for a super-Ohmic bath, the transition occurs only at infinitely strong coupling³⁵. In contrast, in Caldeira-Leggett-type Hamiltonians, dissipation induced squeezing occurs³⁷, which originates from the effect of damping in reducing the rate of escape from a metastable well.

In a linear harmonic oscillator, the ground state wave function is a gaussian. It is natural to ask, to what extent this picture holds in the case of finite electron-phonon coupling. The probability distribution of the oscillator coordinator or displacement reads as

$$j_{\text{osc}}(x)^2 = \langle Q(x) \rangle = \lim_{\alpha \rightarrow 0} \int_{-\infty}^{\infty} \frac{dk}{2} \exp(ik(Q(x) - \alpha k)) i; \quad (17)$$

In the second step, a useful representation of the Dirac-delta function was inserted. Since the Hamiltonian is quadratic, or the corresponding action is gaussian for the phonons after integrating out the fermions, the expectation value of the exponent can be calculated following Ref. 28, which leads to

$$j_{\text{osc}}(x)^2 = \frac{1}{2\langle Q^2 \rangle} \exp \left(-\frac{x^2}{2\langle Q^2 \rangle} \right); \quad (18)$$

The ground state wave function remains gaussian, but the variance ($\langle Q^2 \rangle$) increases monotonically with g . The region where the phonons are mainly restricted to, is

wider than without electron-phonon coupling. The coupling to electron increases the average oscillator displacement around the equilibrium. This further corroborates the picture emerging from the previous studies.

The phonon contribution to the free energy can be calculated by using Pauli's trick of integrating over the coupling constant. After some algebra, one arrives at

$$F = F_e + T \ln 2 \sinh \frac{\omega_0}{2T} \frac{1}{\omega_0^2} + \int_0^\infty \frac{dx}{2} b(x) \tan^{-1} \frac{2x}{\omega_0^2 (1 - (\beta_2 - \beta_+))}; \quad (19)$$

where F_e is the free energy of the fermions in the absence of phonons, $b(x)$ is the Bose distribution function, and the integral should be limited to the bandwidth, but this can be sent to infinity when obtaining quantities by differentiating³⁶. One has to carefully choose the appropriate phase angle of the \tan^{-1} function. This expression is similar to the free energy of the two channel Kondo model in a magnetic field ($\omega_0 \rightarrow 1$ ($\beta_2 = \beta_+$)) here) along the Emery-Kivelson line³⁸, after replacing the Bose distribution function with the Fermi one. However, our "magnetic field" cannot be switched off, hence the entropy is zero at $T = 0$, similarly to the underscreened Kondo model³⁹. The specific heat can be calculated by $C_p(T) = -T(\partial^2 F / \partial T^2)$. Its low temperature ($T \rightarrow 0$ ($\beta_2 = \beta_+$)) behaviour due to phonons reads as

$$C_p(T) = \frac{T}{6v_2}; \quad (20)$$

which sharpens when β_2 is approached. The exponential freezing-out of the Einstein phonon changes to a linear T dependence, and adds to the Sommerfeld coefficient of the conduction electrons, and enhances it. Had we chosen acoustic phonons, their T^3 specific heat would also be overwhelmed at low temperatures. At higher temperatures, a broad bump shows up in the specific heat as a function of temperature due to the presence of g . This can serve as an identifier of the local electron-phonon interaction, and is shown in Fig. 2. Similar structures have been observed in the Anderson-Holstein impurity model by NRG¹¹.

VI. ELECTRONIC PROPERTIES: SUSCEPTIBILITY AND LOCAL DENSITY OF STATES

The phonons are expected to have a profound impact on the electronic properties. Had we integrated them out, we would have arrived to a local dynamic electron-electron interaction, attractive at low energies and repulsive for higher ones. Static interactions already modify significantly the electronic response, as was demonstrated in the Wilson model^{20,30,40}. In the followings we are going

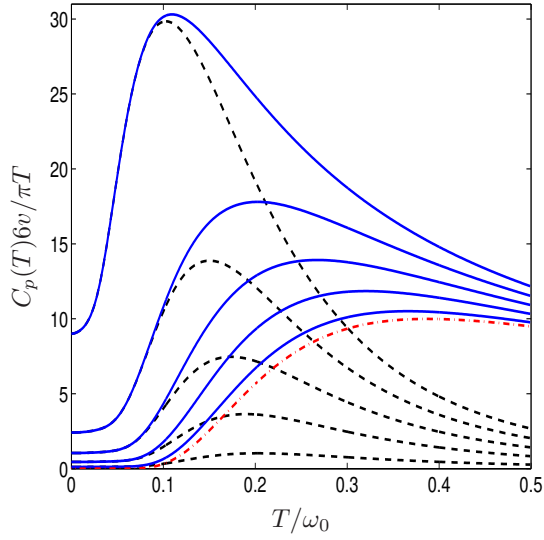


FIG. 2: (Color online) The total (blue solid line) phonon specific heat contribution for different values of the coupling constant $g_2 = 0.1, 0.3, 0.5, 0.7$ and 0.9 , $W = \omega_0 = 10$ from bottom to top. The red dashed dotted line shows the pure phononic $g_2 = 0$ specific heat, while the black dashed curves stands for their difference due to the finite coupling g . Note the sharpening of the broad bump at low T as g increases.

to see the effect of dynamic one explicitly on the electron system.

The electric charge is defined through $\chi(x) = \langle \hat{Q}_x(x) \rangle = \frac{1}{\beta} \ln Z$. The local charge correlation function is evaluated from Eq. (3) using the diagrammatic technique, and along the real frequency axis it reads as

$$\chi_{\text{charge}}(\omega) = \frac{2 \chi(\omega)}{1 + \frac{2g^2}{m(\omega^2 - \omega_0^2)}}; \quad (21)$$

The local charge excitation energies are determined from the poles Eq. (21), which possess finite lifetime, as given by Eq. (14). Eq. (21) is the standard result in the random-phase approximation, which turns out to be the exact one in the present case. Most of the many body contributions are canceled by the Ward identity, which relates the vertex function and the electron propagator. This could be expected from the fact that the model is solvable by bosonization. The very same phenomenon revealed itself during the study of the W ol impurity model^{29,40}. The dynamic nature of the phonons is observable in the denominator of Eq. (21). In the static limit, the effective interaction between the electrons is attractive, and changes to repulsive for frequencies exceeding the phonon energy ω_0 . The static limit of the charge susceptibility simplifies to

$$\chi_{\text{charge}}(0) = \frac{2 \chi^2 W}{(1 - (g_2)^2)}; \quad (22)$$

In accordance with Eq. (14), this also predicts the transition to the distorted phase, which would be accompanied

by the rearrangement of the charges as well. This signals that our model is on the brink of charge Kondo effect. Similar enhancement of the charge response has been reported in Ref. 11.

Since we work with spinless electrons, the single particle Green's function can be evaluated, unlike in the $SU(N)$ Wol model^{20,30} or the two channel Kondo model³⁸. There, such a calculation would involve formally $\langle \chi(x) \rangle$, which is difficult to work with. The local retarded Green's function is defined as

$$G_R(t) = \frac{1}{i} \langle t(t) h f(t); -^+(0) g i \rangle = \frac{1}{i} \langle t(t) \frac{\exp(-4 \hbar^2 i)}{2} [\exp(4 C(t)) + \exp(4 C(-t))] \rangle; \quad (23)$$

where in the second step we made use of the gaussian nature of the action and used the usual tricks of operator manipulation^{27,28}. The task is to evaluate the correlator $C(t) = \langle h(t) \langle 0 | i \rangle$, whose second appearance in Eq. (23) follows from time reversal symmetry. Given the fact that the bosonized Hamiltonian (Eq. (3)) is quadratic, we can evaluate this expectation value at bosonic Matsubara frequencies using the path integral representation of the problem³⁰. Then by transforming it to imaginary times, finally we can read off $C(t)$ after careful analytic continuation to real times. First we find for the Matsubara form that

$$C(i_m) = \frac{1}{4j_m j} + \frac{m}{2} D_Q(i_m); \quad (24)$$

Here the first term is responsible for the $1/\omega$ decay of fermionic correlations. Fortunately, the second expression, accounting for the phonon contribution, is separated from the first one, and does not require ultraviolet regularization unlike the first one, where the large i_m part need to be cut off to avoid divergences.

Compared to the exact expression derived in the atomic limit ($G_{\text{at}}(t)$ in Eq. (8)), Eqs. (23)–(24) have identical structures. It contains the free fermionic contribution, and in addition, the exponentiated phonon Green's function. Since the coupling constant appears in the exponent, together with D_Q , similarly to the exact solution in the atomic limit, this suggests the non-perturbative nature of our bosonization approach in the presence of a finite electron band. Hence we believe, that our study captures correctly the physics in the whole parameter range.

Its Fourier transform with respect to i_m yields to the imaginary time ordered expression for the correlator, from which the desired relation can be obtained as

$$C(t) - C(0) = \frac{1}{4} \ln \frac{1}{1 + i v t} + \frac{m}{2} (D_Q(t) - \hbar^2 i); \quad (25)$$

where the equal time correlator need to be subtracted to regularize the first term on the right hand side and

$$D_Q(t) = \frac{2i}{m(\omega_{p+} - \omega_p)} (f(\omega_{p+} t) - f(\omega_p t)) \quad (26)$$

with

$$f(x) = \sin(x) \text{Si}(x) - \frac{1}{2} \sin(x) \cos(x) \text{Ci}(x); \quad (27)$$

where $\text{Si}(x)$ and $\text{Ci}(x)$ are the sine and cosine integrals. At large times, its decay is characterized by the damping, $\text{Im} \epsilon_p$, and the frequency of oscillations by $\text{Re} \epsilon_p$. By plugging this formula to $G_R(t)$, we evaluate the retarded single particle Green's function. The local density of states follows as

$$\begin{aligned} \rho(\epsilon) &= \frac{1}{\pi} \text{Im} \int_0^\infty dt \exp(i\epsilon t) G_R(t); \\ &= \text{Re} \left[\frac{1}{1 + i \exp(-2m D_Q(t))} \frac{dt \exp(i\epsilon t)}{t} \right]; \quad (28) \end{aligned}$$

It is shown in Fig. 3 for various values of g . As g increases from weak ($g = 0.1$) to strong coupling ($g = 0.9$), the residual density of states decreases monotonically. In addition, increasing amount of spectral weight is transferred away from the central region around $\epsilon = 0$, in perfect agreement with what we found in limiting cases of the model in Sec. III. Complete suppression at $\epsilon = 0$ occurs in all cases at infinitely strong coupling, similarly to the bosonized case at $g = 2$. This is why we believe that our approach captures correctly the strong coupling limit as well. Close to the critical coupling g_c , the density of states exhibits a V-shapes form around the Fermi energy. Similar redistribution of spectral weight was identified in the adiabatic, anti-adiabatic and atomic limit. These findings are also in accordance with those found by NRG in the Anderson-Holstein impurity model^{4,5,16}. There, in the non-interacting version of the model, a resonance peak shows up at the f-level energy, which narrows significantly in the presence of phonons, and increasing amount of spectral weight is transferred away from this region. A more direct comparison is difficult, since the Anderson-Holstein impurity model distinguishes between conduction and localized electrons, which are weakly hybridized with the conduction band, as opposed to our one-band model. Similar reasoning separates the purely electronic Anderson impurity model from the Wilson impurity model⁴⁰.

The significant decrease (dip like structure) in $\rho(0)$ should be detected in point contact spectroscopy or by scanning tunneling microscopy experiments in bulk materials. For small values of g , a steplike drop occurs with decreasing frequency close to $\epsilon = \epsilon_0 - 1 = \epsilon_2$, which smoothens as the electron-phonon coupling increases, through the appearance of other steplike features, as is seen in Fig. 3 for $g = 0.7$. As ϵ_0 increases, the drop in the density of states occurs at higher frequencies ($\epsilon_0 - 1 = \epsilon_2$), and the suppression of the residual density of states at $\epsilon = 0$ is more efficient for higher ϵ_0 , as can be seen in the inset of Fig. 3.

These features are different from that induced by a non-magnetic impurity or by a magnetic one, and the reason is the effective, dynamically attractive interaction generated by the phonons.

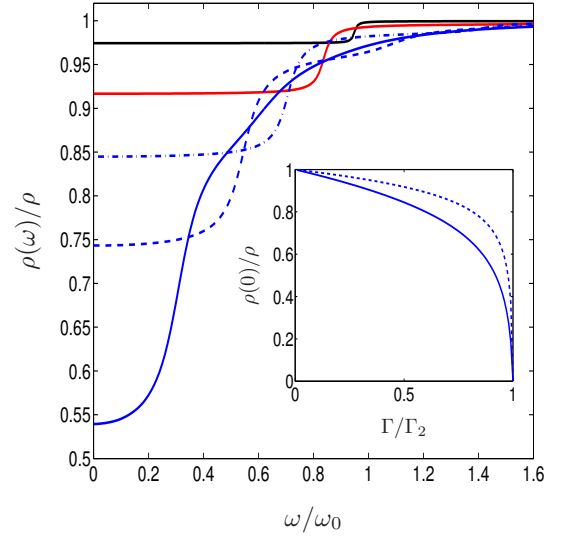


FIG. 3: The change of the local electron density of states at the impurity site is shown for $W = \epsilon_0 = 10$ from weak to strong coupling for $g = 0.1$ (black), 0.3 (red), 0.5 (blue dashed-dotted), 0.7 (blue dashed) and 0.9 (blue solid) from top to bottom. Increasing amount of spectral weight is transferred away from the zero frequency region with g . The inset visualizes the change in the residual density of states for $W = \epsilon_0 = 10$ (solid) and 20 (dashed), which vanishes at $g = 2$.

VII. CONCLUSION

In conclusion, we have studied a model of spinless fermions interacting with an Einstein phonon (single impurity Holstein model) using Abelian bosonization. With increasing coupling, the phonon mode softens, and at $g = 1$, distortion occurs. The softening of the phonon resonance takes place in two steps: first, the frequency starts softening, and acquires finite lifetime. Then oscillations disappear from the response, and two distinct, finite dampings characterize the phonons. Finally, at a critical coupling, which is conjectured to be at $g = 1$, the phonons are distorted. These manifest themselves in the specific heat through the enhancement of the Sommerfeld coefficient. The phonon's entropy is similar to that of the Kondo model in non-magnetic field³⁹, hence vanishes at $T = 0$. The present model resembles closely to the underscreened Kondo model in magnetic field. The local charge susceptibility is strongly enhanced, similarly to the spin susceptibility of the Kondo model. This points toward the realization of charge-Kondo effect. Closed expression is derived for the local electronic density of states. With increasing coupling, significant amount of spectral weight is transferred away from the $\epsilon = 0$ region,

in accordance with results in the atomic limit and in the Anderson-Holstein impurity model. This should be observable in point contact spectroscopy, or on a molecule trapped near a tunnel junction, and influence the current-voltage characteristic as well.

Acknowledgments

We thank P. Fazekas and P. S. Comaglia for useful discussions. This work was supported by the Hungar-

ian Scientific Research Fund under grant number OTKA TS049881.

-
- Electronic address: dora@m-pipks-dresden.mpg.de
- ¹ A. C. Hewson, *The Kondo Problem to Heavy Fermions* (Cambridge University Press, Cambridge, Great Britain, 1993).
 - ² A. O. Gogolin, A. A. Nersisyan, and A. M. Tsvelik, *Bosonization and Strongly Correlated Systems* (Cambridge University Press, Cambridge, 1998).
 - ³ F. D. M. Haldane, *Phys. Rev. B* **15**, 281 (1977).
 - ⁴ A. C. Hewson and D. Meyer, *J. Phys. Cond. Matter* **14**, 427 (2002).
 - ⁵ P. S. Comaglia, H. Ness, and D. R. Gempel, *Phys. Rev. Lett.* **93**, 147201 (2004).
 - ⁶ D. Mozysku and I. Martin, *Phys. Rev. Lett.* **89**, 018301 (2002).
 - ⁷ U. Lundin and R. H. McKenzie, *Phys. Rev. B* **66**, 075303 (2002).
 - ⁸ J.-X. Zhu and A. V. Balatsky, *Phys. Rev. B* **67**, 165326 (2003).
 - ⁹ S. Sanada, Y. Aoki, H. Aoki, A. Tsuchiya, D. Kikuchi, H. Sugawara, and H. Sato, *J. Phys. Soc. Jpn.* **74**, 246 (2005).
 - ¹⁰ S. Yotsuhashi, M. Kojima, H. Kusunose, and K. Miyake, *J. Phys. Soc. Jpn.* **74**, 49 (2005).
 - ¹¹ T. Hotta, *J. Phys. Soc. Jpn.* **76**, 023705 (2007).
 - ¹² L. H. Yu and D. Natelson, *Nano Lett.* **4**, 79 (2004).
 - ¹³ H. Park, J. Park, A. K. L. Lim, E. H. Anderson, A. P. A. Livisatos, and P. L. McEuen, *Nature* **407**, 57 (2000).
 - ¹⁴ A. C. Hewson and D. M. Newns, *J. Phys. C* **12**, 1665 (1979).
 - ¹⁵ A. C. Hewson and D. M. Newns, *J. Phys. C* **13**, 4477 (1980).
 - ¹⁶ G. S. Jeon, T.-H. Park, and H.-Y. Choi, *Phys. Rev. B* **68**, 045106 (2003).
 - ¹⁷ U. Weiss, *Quantum Dissipative Systems* (World Scientific, Singapore, 2000).
 - ¹⁸ A. J. Leggett, S. Chakravarty, A. T. Dorsey, M. P. A. Fisher, A. Garg, and W. Zwerger, *Rev. Mod. Phys.* **59**, 1 (1987).
 - ¹⁹ A. A. Abrikosov, *Fundamentals of the Theory of Metals* (North-Holland, Amsterdam, 1998).
 - ²⁰ P. A. Wolf, *Phys. Rev.* **124**, 1030 (1961).
 - ²¹ M. Capone and S. Ciuchi, *Phys. Rev. Lett.* **91**, 186405 (2003).
 - ²² I. A. A. and A. W. W. Ludwig, *Nucl. Phys. B* **360**, 641 (1992).
 - ²³ P. Coleman and C. Pepin, *Phys. Rev. B* **68**, 220405 (2003).
 - ²⁴ A. Taraphder and P. Coleman, *Phys. Rev. Lett.* **66**, 2814 (1991).
 - ²⁵ R. Zitko and J. Bonca, *Phys. Rev. B* **74**, 224411 (2006).
 - ²⁶ D. Waxman, *J. Phys. A: Math. Gen.* **23**, 1137 (1990).
 - ²⁷ R. Shankar, *Acta Phys. Pol. B* **26**, 1835 (1995).
 - ²⁸ J. von Delft and H. Schoeller, *Ann. Phys. (Leipzig)* **7**, 225 (1998).
 - ²⁹ G.-M. Zhang, *Commun. Theor. Phys.* **34**, 211 (2000).
 - ³⁰ B. Dora, *Phys. Rev. B* **73**, 125113 (2006).
 - ³¹ A. O. Caldeira and A. J. Leggett, *Ann. Phys. (N.Y.)* **149**, 374 (1983).
 - ³² J. E. Hirsch and E. Fradkin, *Phys. Rev. B* **27**, 4302 (1983).
 - ³³ G. D. Mahan, *Many particle physics* (Plenum Publishers, New York, 1990).
 - ³⁴ G. Zarand and J. von Delft, *Phys. Rev. B* **61**, 6918 (2000).
 - ³⁵ R. Silbey and R. A. Harris, *J. Chem. Phys.* **93**, 7062 (1989).
 - ³⁶ M. Fabrizio, A. O. Gogolin, and P. Nozières, *Phys. Rev. Lett.* **74**, 4503 (1995).
 - ³⁷ V. Ambegaokar, *J. Stat. Phys.* **125**, 1187 (2006).
 - ³⁸ V. J. Emery and S. Kivelson, *Phys. Rev. B* **46**, 10812 (1992).
 - ³⁹ P. Schlotmann and P. D. Sacramento, *Adv. Phys.* **42**, 641 (1993).
 - ⁴⁰ P. Schlotmann, *Phys. Rev. B* **17**, 2497 (1978).